J. Fluid Mech. (1974), *vol.* 66, *part* 1, *pp.* 67–79
Printed in Great Britain

Oscillatory and collective instabilities in large Prandtl number convection

By F. H. BUSSE AND J. A. WHITEHEAD†
Institute of Geophysics and Planetary Physics, University of California, Los Angeles

(Received 10 December 1973 and in revised form 29 March 1974)

An experimental study of transitions from steady bimodal convection to time-dependent forms of convection is described. Using controlled initial conditions for the onset of bimodal convection two mechanisms of instability can be separated from the effects of random noise. The oscillatory instability of bimodal cells introduces standing waves closely resembling those occurring in low Prandtl number convection. The collective instability introduces spoke-pattern convection which is characteristic for turbulent large Prandtl number convection. Both instabilities originate primarily from the momentum advection terms in the equations of motion, as is evident from the strong Prandtl number dependence of the critical Rayleigh number R_t for the onset of oscillations. The results are discussed in relation to previous experiments and recent theoretical work.

1. Introduction

Among hydrodynamic systems exhibiting the phenomenon of turbulence, convection in a layer heated from below possesses unique properties. Because of the simple gravitational mechanism of instability the physical conditions depend only on the vertical co-ordinate. Thus turbulent convection is distinguished among other cases of turbulence by the property that it is statistically stationary in time as well as isotropic and homogeneous with respect to two spatial dimensions. The absence of a mean flow has the additional consequence that the centre of mass of any horizontal sublayer of fluid remains stationary with respect to the laboratory frame of reference. This is important from the experimental point of view since turbulent processes can be observed in their local frame of reference. On the other hand, convection may appear to be more complicated than purely hydrodynamic turbulence owing to the presence of thermal effects. A detailed inspection of the basic Boussinesq equations of convection shows, however, that the additional temperature variable is mathematically analogous to the velocity variables and does not complicate the solution of the equations. Thus it is not surprising that convection in a layer heated from below has become one of the principal cases in experimental and theoretical research on turbulent processes.

The simple properties of convection and the convenience of experimental

† Present address: Woods Hole Oceanographic Institution, Woods Hole, Massachusetts.

observation are responsible for the fact that more regular features are seen in convection than in other cases of flows generated by instabilities. At low Rayleigh numbers convection exhibits a variety of steady flows, and even at higher Rayleigh numbers when time-dependent processes occur distinct frequencies are observed. The transition to increasingly more turbulent motion occurs by discrete steps. These steps represent instabilities by which a more complex form of motion replaces a less complex flow as the Rayleigh number increases. Starting with the basic static state as the solution of highest symmetry of the problem the first transition, representing the onset of convection, introduces two-dimensional motions in the form of periodic rolls. Three-dimensional forms of convection replace the two-dimensional rolls in the second transition. At high Prandtl number this transition leads to bimodal convection, which has been investigated in detail theoretically and experimentally (Busse 1967; Krishnamurti 1970*a*; Busse & Whitehead 1971). At moderate and low Prandtl numbers, say less than about 5, oscillatory convection occurs with waves propagating along the axes of convection rolls. Recent experiments (Willis & Deardorff 1970) and theoretical work (Busse 1972; Clever & Busse 1974) have led to a good understanding of this process.

Bimodal convection shares with two-dimensional convection rolls the property that it is steady. Hence a special importance is attached to the third transition, which, at high Prandtl number, introduces time dependence for the first time. Although a number of observations of this transition have been reported (Rossby 1966; Willis & Deardorff 1967; Krishnamurti 1970*b*, 1973), the origin of the instability has remained a subject of controversy. While Krishnamurti finds that the critical Rayleigh number R_t for the onset of time-dependent convection becomes independent of the Prandtl number P as P exceeds a value of order 50, Willis & Deardorff (1970) suggest that the instability is similar to the oscillatory instability at low Prandtl number. In this case a strong dependence of R_t on the Prandtl number must be expected since the oscillations originate from the momentum advection terms in the equations of motion (Busse 1972). In this paper we shall present experimental evidence for the latter interpretation. The discrepancy with the findings of Krishnamurti will be resolved by the fact that the onset of oscillations is very sensitive to inhomogeneities in the convection pattern. Since those inhomogeneities are always present in an experiment started from random initial conditions, oscillations indeed appear first at isolated spots as observed by Krishnamurti. If, however, initial conditions are chosen such that a regular convection pattern is established, the onset of oscillations occurs homogeneously at a Rayleigh number R_t increasing approximately linearly with Prandtl number.

Another instability to be studied in this paper is the collective instability leading to spoke-pattern convection. It differs from the other known instabilities in that it introduces a subharmonic wavenumber. Several bimodal cells are combined into one cell characterized by a spoke structure. Spoke patterns of ascending or descending fluid sheets represent a characteristic feature of turbulent convection at high Prandtl number. The generation of this pattern in a regular manner demonstrates its quality as a distinctive form of convection.

The results of this paper together with those of our earlier paper Busse & Whitehead 1971, to which we shall refer as I) emphasize the importance of experiments with controlled initial conditions for the understanding of turbulent processes. As we shall outline in more detail at the end of the paper, two major effects present in the general case of turbulent convection can be separated: the randomness caused by initial conditions or small inhomogeneities and the discrete transitions introducing flows with qualitatively new features. Because of the existence of a large manifold of possible solutions, randomness in initial and other conditions of the problem becomes amplified and does not die away as in the case when the static solution is unique. By eliminating random influences the nature of the transitions can be clearly exhibited. This is the goal of the experiments described in this paper.

The paper starts with a description of the experimental procedure in §2. The observations of oscillatory instability are discussed in §3. The theoretical solutions for the closely related oscillations of rolls prove to be helpful in explaining various observed features. No related theory is available in the case of the collective instability which is described in §4. The paper closes with some remarks which attempt to demonstrate the relevance of the results to more general ideas on turbulence.

2. Experimental technique

The experimental apparatus and the method of observation have been described in I and only a brief description will be given here as shown in figure 1. A horizontal layer of silicone oil is bounded above and below by plate-glass water jackets connected to thermostatic baths. The jackets are carefully levelled and kept parallel. Convection is observed in a region with a horizontal extent 80×80 cm. This region is bounded laterally by Plexiglas inserts which are sandwiched between the upper and lower jackets.

The convection pattern is visualized by a shadowgraph method. A slightly diverging beam of light from a point source traverses the convection layer before meeting the screen. Owing to the temperature differences between upward and downward motions the convection pattern acts like a lens. Bright lines on the screen are caused by the focusing effect of descending sheets of cold fluid. Dark areas correspond to hot fluid elements. Silicone oils of Dow Corning '200' type were used in all experiments. Properties taken directly or interpolated from Dow Corning data are given in table 1 for the four different sets of experiments. We shall refer to the four different cases by their Prandtl number.

The initial conditions for the onset of convection were controlled by using the inducing procedure developed by Chen & Whitehead (1968) and used in I. A grid consisting of regularly spaced tapes stretching across a frame is placed on top of the upper glass jacket and light is shone downwards through the grid into the convection layer while it is in its stable static state. The absorption of radiation gives rise to a small temperature increase ($\approx 0{\cdot}05\,^{\circ}\mathrm{K}$) along the strips of illuminated silicone oil. After a period of several thermal time scales d^2/κ, where d refers to the depth of the convection layer and κ is the thermal diffusivity, the

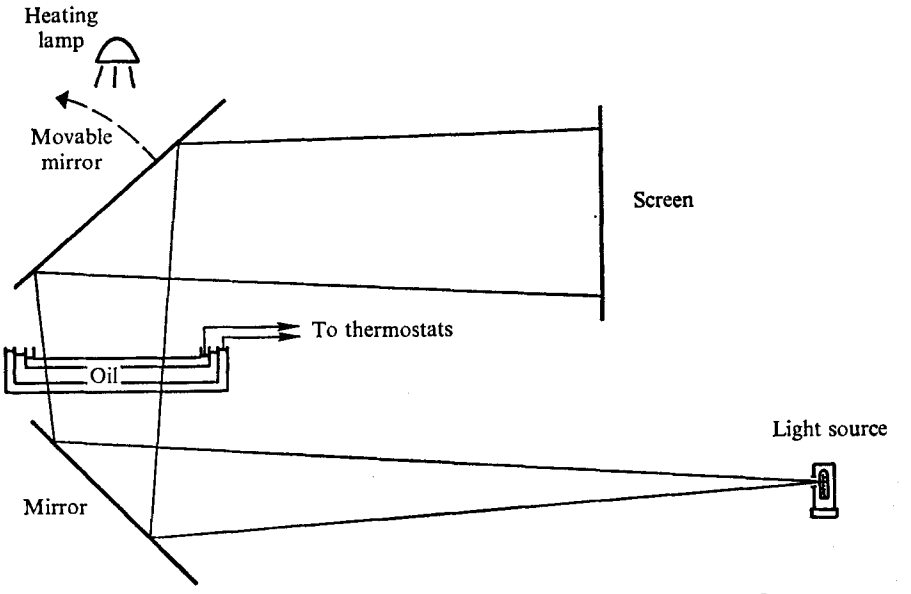

FIGURE 1. Qualitative sketch of experimental apparatus and method of observation.

Prandtl number P	Kinematic viscosity (centiStokes)	Thermal diffusivity ($cm^2 s^{-1} \times 10^{-4}$)	Thermal expansion coefficient ($°C^{-1} \times 10^{-3}$)	Layer depth d (cm)
16	1·0	6·1	1·34	0·55
46	3·1	6·7	1·06	1·0
63	4·4	7·0	1·06	1·3
126	10·0	7·9	1·08	2·0

TABLE 1. Properties of Dow Corning '200' silicone oils used as convection fluids taken and interpolated from *Dow Corning Bull.* no. 05-172.

second stage of the experiment is started by raising the temperature in the lower water jacket and reducing it in the upper jacket at a rate of about 0·3 °K/min. Shortly thereafter the heating lamp is turned off, the grid is removed and the observation of the convection by shadowgraph visualization is started. In order to obtain optimal images on the screen, the depth d of the convection layer was selected to give the desired Rayleigh number with 3 cm °K $\lesssim d\Delta T \lesssim$ 12 cm °K.

In I the method described above was used to investigate the instabilities of regular convection rolls including the onset of bimodal convection caused by the cross-roll instability. Since we are concerned in the present experiment with the instability of bimodal convection, it becomes important to have a regular pattern of this form of convection. Hence, a number of experiments were carried out with cross-rolls of the desired wavelength induced in a similar manner to that for the original rolls. For this purpose a grid with the appropriate spacing is placed at right angles to the previously generated rolls while the Rayleigh

number is kept at a value of about 2×10^4. The heating lamp is turned on for an interval of about one thermal time constant, after which the experiment proceeds in the manner described above. The experiments shown in figures 7–9 (plates 3–5) were performed in this way. Because of the finite size and the finite distance of approximately 1·5 m of the heating lamp the induced wavenumbers may vary by a few per cent through the convection layer.

The observations were recorded by taking photographs at suitable intervals, and in the case of oscillatory convection, time-lapse movies were taken at speeds of 8, 16, 24 and 40 frames/min. In general the screen was used in a position in which it intersected the light beam at an oblique angle. In this way the cameras could be placed normal to the screen without interfering with the light beam. Hence the length scale in the direction of the long side of the photographs shown on the plates is elongated by a factor which can be obtained by comparing the ratio of the observed wavelengths of bimodal cells with those given in the figure captions.

For the calculation of Rayleigh numbers from measured temperature differences between the water jackets, it was necessary to make corrections for the temperature gradients in the glass plates above and below the convection layer. Since the heat flux was not measured in this experiment and since theoretical values for the heat transport by bimodal convection are not available, the following dependence of the Nusselt number on the Rayleigh number was assumed:

$$Nu = 0{\cdot}19R^{0{\cdot}282}. \tag{2.1}$$

Relation (2.1) represents an average of the data of Rossby (1966) and Somerscales & Gazda (1969) for Rayleigh numbers of order 10^5 and Prandtl numbers between 20 and 200. Because of the indirect method of correction and because of uncertainties in the material properties it is estimated that the accuracy of the Rayleigh numbers is of the order of 5 %.

Relation (2.1) also indicates that for Rayleigh numbers of order 10^5 the effective heat conductivity of the convection layer is five times larger than in the static state. This explains the rapid adjustment of the convection to changes in the applied temperature. Accordingly, the requirements for quasi-stationarity in changes of the applied temperature difference are considerably lowered at high Rayleigh numbers.

3. Transition to oscillatory convection

Although numerous experimental investigators have paid particular attention to the first appearance of time-dependent effects in a convection layer under steady conditions, the onset of oscillations and their origin is still a controversial topic. The problem appears to be understood best in the case of low Prandtl number fluids, where oscillations are associated with the instability of two-dimensional convection rolls. The relatively simple nature of the instability has permitted a theoretical solution in the case of free (Busse 1972) and rigid boundaries (Clever & Busse 1974). In agreement with observations of convection in air by Willis & Deardorff (1970), the solution shows that the oscillations correspond to waves propagating along the axis of the rolls while shifting the rolls forwards

and backwards in the perpendicular horizontal direction. At Prandtl numbers above the order of 5 the oscillatory instability of rolls cannot be realized because it is preceded by the transition to bimodal convection. The latter can be visualized roughly as the superposition of two roll patterns with different wavelengths at right angles. Since the homogeneity along the axis of the basic rolls is lost in the case of bimodal convection, propagating waves can no longer be expected. Standing waves may be expected, however, and are indeed observed. Figure 2 (plate 1) shows first the transition to bimodal convection and then the onset of oscillations in the form of standing waves on the boundary of the short wavelength component of the bimodal convection. Since the dissipation rises rapidly with the wavenumber of the oscillation, waves on the large wavelength or basic component of bimodal convection do not occur. In order to give some impression of the time dependence of the oscillation, opposite phases have been photographed in figures 2(*e*) and (*f*) and in some of the following figures. Although the phase of the oscillation varies across the convection layer, its frequency is fairly constant according to the observations as is also borne out by the consistent change in phase shown in figures 2(*e*) and (*f*). We note that a larger than normal rate of increase in Rayleigh number has been chosen for some of the sequences of photographs in order to show the development of different stages of convection in an optimal way. The rate of change was still low enough, however, not to alter noticeably the convection flow.

As the Prandtl number is increased, the appearance of the waves changes gradually to resemble more a pulsating blob. Although discrete values of P are used in the experiment, we wish to emphasize the word 'gradually' since even at a given Prandtl number P the appearance exhibits a similar change as the wavenumber α_2 of the short wavelength component is increased in small steps. Figure 7 (plate 3), for example, still shows a wavy boundary at the Prandtl number $P = 63$ while figure 9 (plate 5) shows typical blob pulsations at the same Prandtl number for a higher value of α_2. Figure 8 (plate 4) shows an intermediate case. In the case $P = 126$ only pulsations were observed as shown in figure 11 (plate 7). The change in appearance may be partly caused by a change in Rayleigh number since the critical Rayleigh number R_t for the onset of regular oscillations increases both with Prandtl number and with the wavenumber α_2. The lowest value of R at which oscillations were observed as a relatively homogeneous regular pattern has been plotted in figure 3 as a function of P. Because of the dependence of R_t on α_2 and because of the limited number of grids available in the experiment, the minimum value of R_t is not well determined by this procedure and considerable scatter is to be expected. The main feature is the strong dependence of R_t on the Prandtl number, which contrasts with the observation of oscillations in an irregular pattern by Krishnamurti (1970*b*) for the same range of Prandtl numbers. Before we comment on this discrepancy we should like to mention that a linear relationship

$$R_t = 2{\cdot}5 \times 10^3 P \tag{3.1}$$

seems roughly to fit the data. The theory of the oscillatory instability of rolls suggests that the onset should depend mainly on the velocity amplitude measured

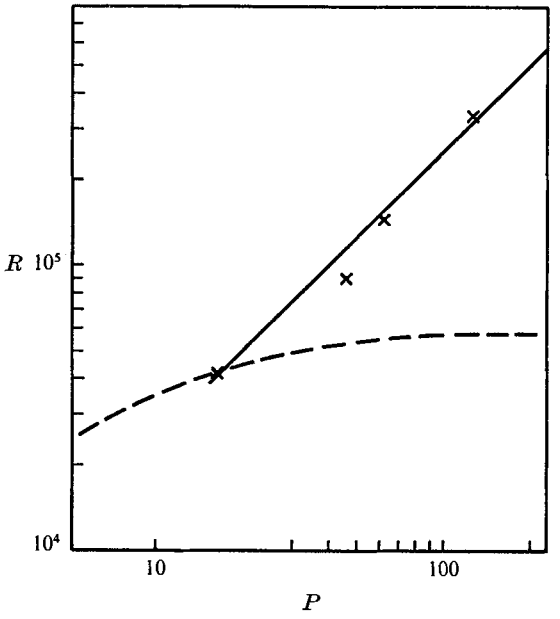

FIGURE 3. Rayleigh number R_t for the transition from regular steady bimodal convection to regular oscillating convection. ---, first occurrence of oscillations in convection started from random initial conditions (from Krishnamurti 1970*b*).

in units of ν/d. Assuming that the Rayleigh number dependence of the amplitude of the secondary component of bimodal cells is the same as that of small amplitude rolls, we find

$$R_t - R_{\mathrm{II}} \propto P^2, \tag{3.2}$$

where $R_{\mathrm{II}} \approx 2{\cdot}3 \times 10^4$ is the Rayleigh number for the onset of bimodal cells. It is evident from the data that they do not contradict a relation of the form (3.2) although an exponent of 1·7 instead of 2 would give the best fit.

The dependence of R_t on the wavenumber α_2 is shown in figure 4. No regular oscillations were observed when α_2 was increased beyond a certain limit, which may depend on P and was not investigated in detail. Figure 9 (plate 5) shows an example in which the wavenumber α_2 is rather large and a transition to spoke-pattern convection takes place without first exhibiting oscillations.

Some observations of oscillations were also made in the case when convection was started from random initial conditions. In agreement with Krishnamurti's (1970*b*) results it was found that oscillations occur at much lower Rayleigh numbers than those given by (3.1) in isolated spots at which the convection pattern is particularly inhomogeneous. In some cases oscillations were even observed at values of R below the transition line plotted by Krishnamurti. Since the occurrence of oscillations appears to depend on the degree of inhomogeneity of the convection pattern, it seems that a sharp value of the Rayleigh number at which oscillations first occur cannot be expected. The strongly Prandtl number dependent onset of oscillations found by Willis & Deardorff (1967) emphasizes this point.

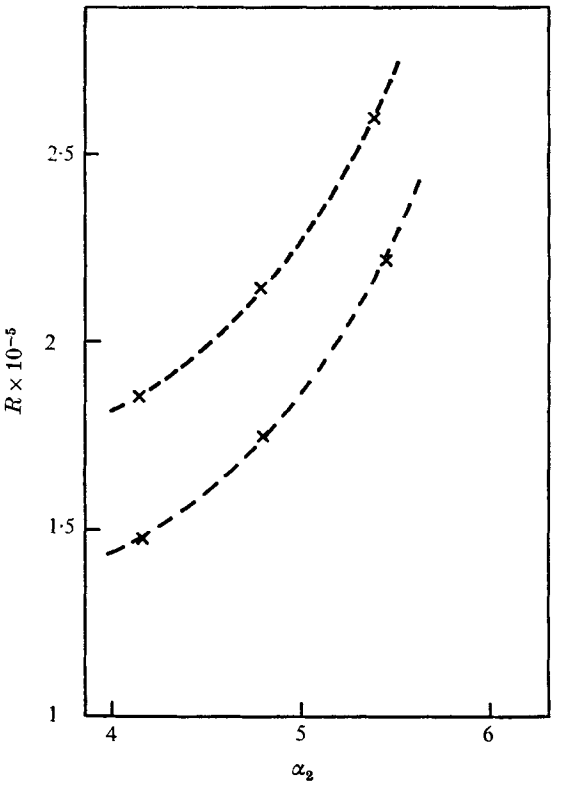

FIGURE 4. The dependence of the Rayleigh number R_t for the onset of regular oscillations on the wavenumbers α_1 and α_2 of bimodal convection in the case $P = 64$. The upper curve corresponds to $\alpha_1 = 2{\cdot}40$, the lower to $\alpha_1 = 2{\cdot}04$.

An easily measurable property of regular as well as irregular oscillations is the period τ. The observed periods made dimensionless by the thermal time constant have been plotted in figure 5. Periods of regular oscillations of bimodal cells are shown as well as periods corresponding to oscillations in irregular patterns. Some data obtained for lower Prandtl numbers have not been included. They continue to fall along the line indicated by the data at the upper left of the graph. Within the scatter of the data the periods agree with those observed by Rossby (1966) and Krishnamurti. Rossby has pointed out that a power law of the form

$$\tau \propto R^{-\frac{2}{3}} \tag{3.3}$$

fits the data well. This power law can be derived for Howard's (1966) simple model of a periodically unstable thermal boundary layer. The Prandtl number dependence of the onset of oscillations does not favour Howard's model since the thermal boundary should be fairly independent of Prandtl number as is indicated by the heat transport. The observations by Krishnamutri (1970*b*) and the theory by Busse (1972) agree on the fact that the oscillation period corresponds to the circulation time of fluid elements in the convection cell. Since the velocity amplitude increases with Rayleigh number, the period must decrease

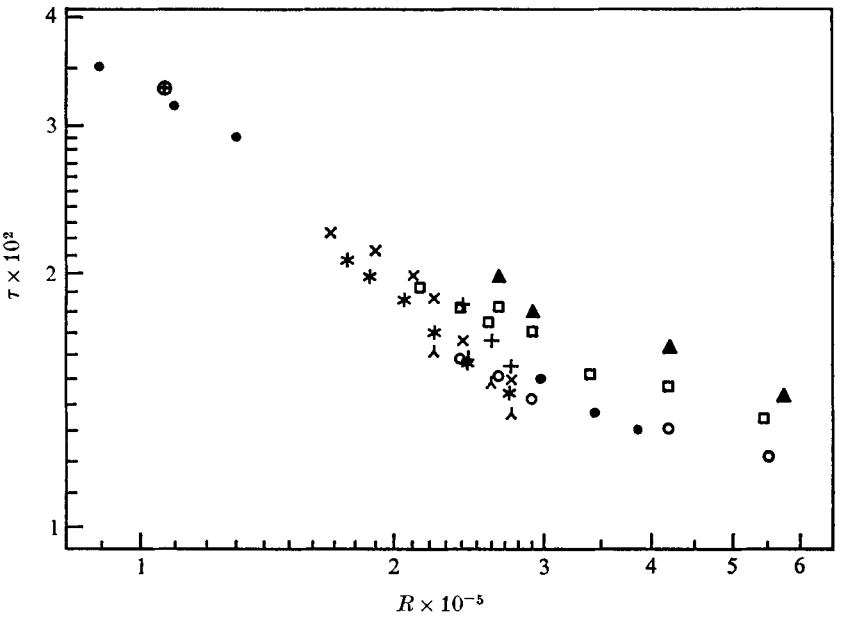

FIGURE 5. Period τ of oscillations based on the thermal time scale κ/d^2 as a function of Rayleigh and Prandtl number. Regular oscillations are given as function of the bimodal wavenumbers (α_1, α_2). $P = 126$: ▲, (2·1, 4·2); □, (2·54, 4·2); ○, (3·1, 4·2). $P = 63$: ✱, (2·40, 4·08); ×, (2·04, 4·8); +, (2·04, 5·45); ⅄, (2·4, 4·8). Irregular oscillations: ●, $P = 63$; ⊕, $P = 44$.

and a power law of the form (3.3) may well be expected. This interpretation is also in agreement with the most obvious feature of the measured oscillation periods, namely their independence of the Prandtl number. Experimental measurements (Deardorff & Willis 1967) and theoretical solutions (Clever & Busse 1974) indicate that the velocity amplitude based on the thermal time scale depends little on the Prandtl number P for $P \gtrsim 1$. Hence, it is not surprising that the period of oscillation is relatively independent of the Prandtl number. The periods observed by Willis & Deardorff (1970) in air appear to contradict this property when compared with the periods observed in water by Krishnamurti (1970*b*). This disagreement can be explained, however, by the fact that oscillations in air occur as an instability of convection rolls, while oscillations in water are preceded by the transition to bimodal convection. Hence the difference in wavenumber rather than a change in the mechanism explains the difference between air and water.

A considerable effort has been made to determine the dependence of the periods of regular oscillations on the wavenumbers α_1 and α_2 of the bimodal cells. The data of figure 5 show that the dependence on α_1 is not negligible. The period tends to increase considerably with the wavelength of the oscillations, which is given by the wavelength $\lambda_1 = 2\pi/\alpha_1$ of the basic mode in the bimodal convection. There seems to be little dependence on the wavenumber α_2. A comparison with the theoretical calculations of Clever & Busse (1974) shows that a similar dependence on the wavenumbers is exhibited by the oscillations of convection rolls. This tends to emphasize the interpretation given above that oscillating bimodal

convection can be regarded as a standing wave on the boundary of the second mode with a wavelength given by the first mode for which the theory of oscillating convection rolls applies qualitatively. The change in appearance of the oscillations as the Prandtl number and the Rayleigh number increase indicates a modifying influence of the thermal boundary layer. A process like that envisioned by Howard (1966) may contribute to the oscillatory instability. The smooth dependence of the measurable parameter suggests, however, that for the Prandtl numbers investigated in the experiment the origin of the oscillations is predominantly the same as in the case of low Prandtl number convection.

A secondary property of the oscillations is the correlation length of the phase of oscillation. This length became remarkably large in some experiments although the phases never became coincident over the entire domain of regular oscillations. Instead the phase of oscillation gave the impression of a large-scale wave propagating in the direction of the basic rolls as shown in figures 9(*b*)–(*f*). There appeared to be little relation between the wavelength of the phase correlation and and the wavelength of the collective instability to be discussed in the following section.

4. Transition to spoke-pattern convection

The experimental results presented in the preceding section clearly demonstrate that the onset of the oscillating instability is very sensitive to small inhomogeneities. This property is even more true for the collective instability which effects the transition to spoke-pattern convection. We have chosen the term 'collective' since between three and six bimodal cells are collected by this instability into one large cell of spoke-pattern convection as shown in figures 6–10 (plates 2–6). The mechanism of this instability is of particular interest since it represents a subharmonic response of the convection system. A new wavenumber several times smaller than the basic wavenumber α_2 in the same direction appears. This contradicts the intuitive notion that increasingly higher wavenumbers are introduced in the transition to turbulence. Since no theoretical analysis of spoke-pattern convection or of a similar subharmonic response in other situations is available, we have to restrict ourselves to a purely phenomenological description.

Although the onset of collective instability is triggered most often by inhomogeneities, the observations also indicate that the instability occurs when the amplitude of regular oscillations of bimodal cells exceeds a certain amplitude. In fact, as is evident from figure 6, the collective instability appears to set in first in places where the amplitude of oscillations is largest. Although the details of the collective instability vary with the wavenumber α_2, it generally starts with a modulation of the amplitude of oscillation. When the amplitude of oscillation of a particular cell is sufficiently large it combines with the neighbouring cells on the same basic roll. A spoke structure is formed when the knots corresponding to the intersections of the bimodal cells with the basic rolls gravitate towards a common centre on the boundary of the basic rolls. The boundaries of the short wavelength mode form the spokes while continuing to oscillate at roughly the

same frequency. The spacing of the spoke pattern is surprisingly regular even though individual spoke structures vary considerably, and the oscillations of spokes tend to have a random phase. The form of the oscillations also shows considerable variation and looks sometimes more like a 'breathing blob', at other times more like a 'waving sheet'. The shadowgraph method emphasizes the dark spokes which correspond to hot sheets of rising fluid. In each of the centres between four dark spoke structures there is, however, a light spoke structure of falling sheets of cold fluid.

Unlike steady bimodal cells, oscillating bimodal cells cannot be generated in a strictly homogeneous pattern. Because of the sensitivity of the collective instability to small inhomogeneities no attempt was made to determine a critical Rayleigh number for the onset of this instability. It appears, however, that this Rayleigh number is close to R_t since the amplitude of oscillations tend to increase rapidly with Rayleigh number.

It was not always possible to observe the collective instability as a relatively homogeneous phenomenon. In cases for large values of α_2 and P for which the Rayleigh number R_t for the onset of oscillations is relatively high, disturbances propagating in from the boundaries introduced spoke-pattern convection before the oscillations became large enough to be unstable with respect to the collective instability. Those cases are shown in figures 9 and 10. In the case of figure 10, even the oscillatory instability did not set in in a homogeneous form because the bimodal pattern disintegrated into spoke-pattern convection before the critical value R_t of the Rayleigh number was reached. Hence it could not be demonstrated that the oscillatory instability will necessarily occur in the case of high values of α_2, as a homogeneous phenomenon. The oscillations associated first with inhomogeneities of the bimodal pattern and later with the spoke structure were observed in this case just as described above.

Because of disturbances propagating in from the side boundaries of the convection layer and because of inhomogeneities in the pattern itself, the regular spacing of spoke-pattern convection tends to disappear within a period of several thermal time constants. As is shown in the last pictures of figures 8 and 9, a random spoke pattern is established in which individual spokes change in time with the oscillation period while the larger-scale structure continues to change on a much longer time scale. The pattern is indistinguishable at this stage from the pattern of convection started from random initial conditions, which exhibits spoke-like structures at Rayleigh numbers considerably below R_t. Our observations agree in this respect with those reported by Willis & Deardorff (1970) for the case $P = 57$.

Spoke structures are ubiquitous in turbulent high Prandtl number convection at high Rayleigh number. They persist as relatively steady features in a randomly oscillating environment. The organization of sheets and plumes of falling and rising fluid in a system of spokes appears to make the convective heat transport more effective. Whether primarily dynamical effects are responsible for the spoke structure, as suggested by the Prandtl number dependence of the transition from bimodal convection, or whether thermal effects are equally important cannot be decided on the basis of the present evidence. The general conclusion can be drawn,

however, that in a system increasingly characterized by small-scale phenomena originating from thin thermal boundary layers, large-scale patterns persist as a dominant feature.

5. Concluding remarks

In the experiments described in this paper and in I we have exhibited four different kinds of spatially periodic convection flows, each of which represents a stable solution of the convection problem for consecutive ranges of the Rayleigh number. Each solution is characterized by a new degree of freedom. Three-dimensional convection in the form of bimodal cells replaces two-dimensional convection rolls. Time-dependent convection is introduced by oscillating bimodal convection. After the flow has become dependent on all four of the basic dimensions, a new subharmonic wavenumber is introduced by spoke-pattern convection. While the occupation of all available degrees of freedom by turbulent motion is a well-recognized idea, the discrete transitions by which this is accomplished differ drastically from the concept of random processes generally assumed in theories of turbulence. Undoubtedly, random processes are as important in thermal convection as in other cases of turbulence. However, they tend to modify the properties of discrete, qualitatively different solutions rather than to dominate the development of turbulence exclusively. We shall try to explain this in the following.

Because of the many degrees of freedom realized in convection flow, the manifold of solutions is greatly increased even if only those solutions which are stable with respect to infinitesimal disturbances are counted as physically significant. Convection rolls show a one-dimensional continuum of stable solutions in the wavenumber space in addition to the continuum of possible horizontal orientations (Busse 1967). Bimodal convection exhibits a two-dimensional continuum in wavenumber space (Whitehead & Chan 1974), and the manifold of realizable spoke-pattern convection flows may be even larger. Because of the large spectrum of available solutions it is not surprising that complex random patterns are realized in general from uncontrolled initial conditions, and that a small amount of noise in the experimental conditions causes continuous variations of the convection pattern. Thus the realizability of a continuum of solutions occupying all major degrees of freedom tends to amplify small amounts of noise, while in the case when the statistically stationary solution is unique, i.e. in the case of the static solution for $R < 1708$, the experimental noise is depressed.

Since the amplification of random noise in ordinary experiments on turbulence tends to obscure the qualitative differences in turbulent flows in different ranges of the external parameters, experiments with controlled initial and boundary conditions are of particular importance. We believe that the convection experiment described in this paper can serve as a model in this respect for the general problem of turbulence. By separating the properties of the discrete transitions from the randomizing effects of noise, the importance of both effects in general cases of moderately turbulent convection has been demonstrated. Moreover, the results presented here together with the evidence of discrete transition in the

turbulent heat transport (Malkus 1954) suggest that both effects are of comparable importance in general cases of turbulence. While convection allows a relatively simple experimental investigation, new observational methods may demonstrate in the future the interaction of both elements of turbulent flow in other cases of turbulence.

The point we intended to make in the above discussion can be illustrated by an analogy from solid-state physics. From the photographs shown in this paper and in I the similarity between the pattern of bimodal convection and a two-dimensional crystal lattice is quite striking. This similarity includes various kinds of irregularities found in the lattice such as edge dislocations. Figure 2(*c*) shows some typical examples. The phenomenological analogy between the crystal structure and convection patterns suggests a physical analogy. The transitions in convection can be seen to correspond to phase transitions from one kind of lattice structure to another. It is well known in solid-state physics that both phase transitions and random lattice irregularities profoundly influence the properties of solids, such as electrical conductivity. Similarly, the heat transport in turbulent convection depends on transitions from one type of convection to another as well as on random effects. Thus an analogy can be seen between the microscopic physics of the solid state and the more complex problem of turbulence.

The research reported in this paper was supported by the Atmospheric Science Section of the National Science Foundation under Grants GA-19605 and GA-31247.

REFERENCES

BUSSE, F. H. 1967 *J. Math. & Phys.* **46**, 410.
BUSSE, F. H. 1972 *J. Fluid Mech.* **52**, 97.
BUSSE, F. H. & WHITEHEAD, J. A. 1971 *J. Fluid Mech.* **47**, 305.
CHEN, M. M. & WHITEHEAD, J. A. 1968 *J. Fluid Mech.* **31**, 1.
CLEVER, R. M. & BUSSE, F. H. 1974 *J. Fluid Mech.* **65**, 625.
DEARDORFF, J. W. & WILLIS, G. E. 1967 *J. Fluid Mech.* **28**, 675.
HOWARD, L. N. 1966 In *Proc. 11th Int. Cong. Appl. Mech.*, pp. 1109–1115. Springer.
KRISHNAMURTI, R. 1970*a* *J. Fluid Mech.* **42**, 295.
KRISHNAMURTI, R. 1970*b* *J. Fluid Mech.* **42**, 309.
KRISHNAMURTI, R. 1973 *J. Fluid Mech.* **60**, 285.
MALKUS, W. V. R. 1954 *Proc. Roy. Soc.* A **225**, 185.
ROSSBY, T. 1966 Dissertation, M.I.T.
SOMERSCALES, E. F. C. & GAZDA, I. W. 1969 *Int. J. Heat Mass Transfer*, **12**, 1491.
WHITEHEAD, J. A. & CHAN, G. L. 1974 To be submitted to *J. Geophys. Fluid Dyn.*
WILLIS, G. E. & DEARDORFF, J. W. 1967 *Phys. Fluids*, **8**, 2225.
WILLIS, G. E. & DEARDORFF, J. W. 1970 *J. Fluid Mech.* **44**, 661.

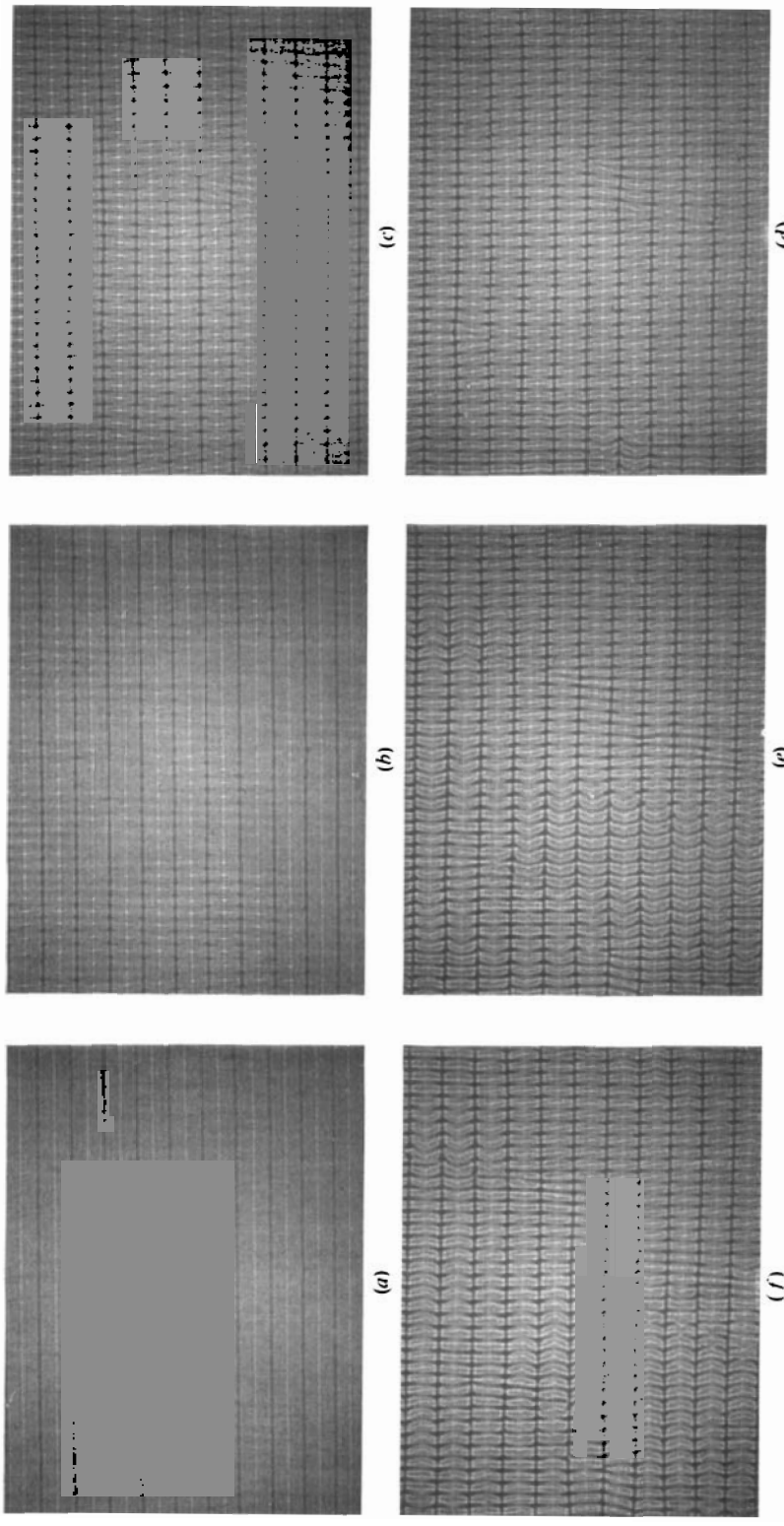

FIGURE 2. Onset of steady bimodal convection ($\alpha_1 = 2{\cdot}3$, $\alpha_2 \approx 5{\cdot}9$) and oscillations for $P = 16$. Time intervals (min): (*a*)–(*b*) 2, (*b*)–(*c*) 10, (*c*)–(*d*) 10, (*d*)–(*e*) 8, (*e*)–(*f*) 2. Rayleigh numbers: (*a*) $3{\cdot}2 \times 10^4$, (*b*) $3{\cdot}6 \times 10^4$, (*c*) $4{\cdot}0 \times 10^4$, (*d*) $5{\cdot}3 \times 10^4$, (*e*) $6{\cdot}1 \times 10^4$, (*f*) $6{\cdot}1 \times 10^4$. Note opposite phase of oscillations in (*e*) and (*f*).

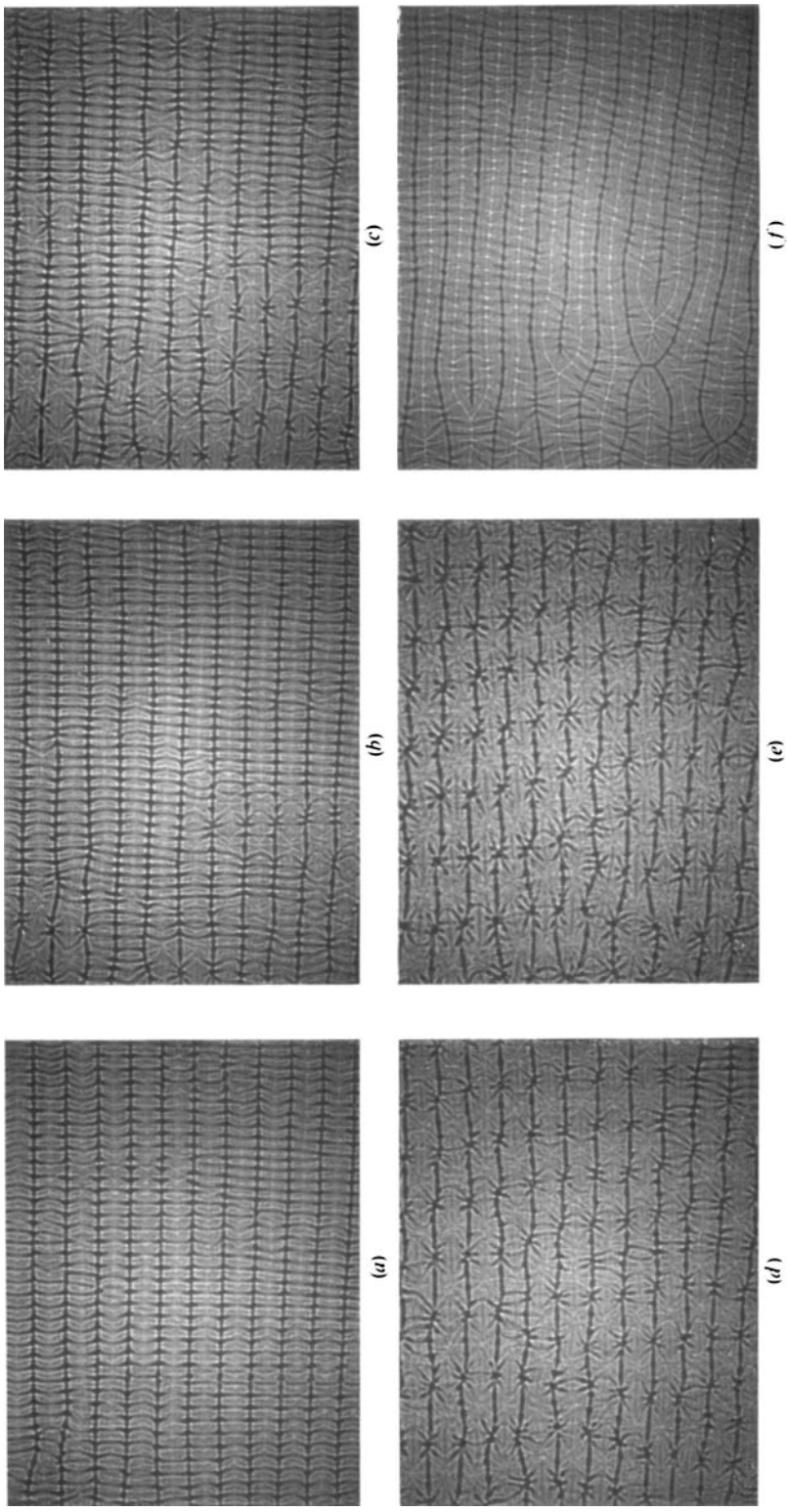

FIGURE 6. Collective instability leading to spoke-pattern convection in the case $P = 16$. Time intervals (min): (*a*)–(*b*) 2, (*b*)–(*c*) 4, (*c*)–(*d*) 10, (*d*)–(*e*) 17, (*e*)–(*f*) 30. Rayleigh numbers: (*a*) $6{\cdot}5 \times 10^4$, (*b*) $6{\cdot}7 \times 10^4$, (*c*) $7{\cdot}2 \times 10^4$, (*d*) $7{\cdot}7 \times 10^4$, (*e*) $9{\cdot}0 \times 10^4$, (*f*) $4{\cdot}0 \times 10^4$. (*a*) shows oscillatory bimodal convection with the first indications of collective instability. The instability progresses in pictures (*b*)–(*d*) and the transition to spoke-pattern convection is essentially completed in (*e*). (*f*) indicates that the transition is reversible.

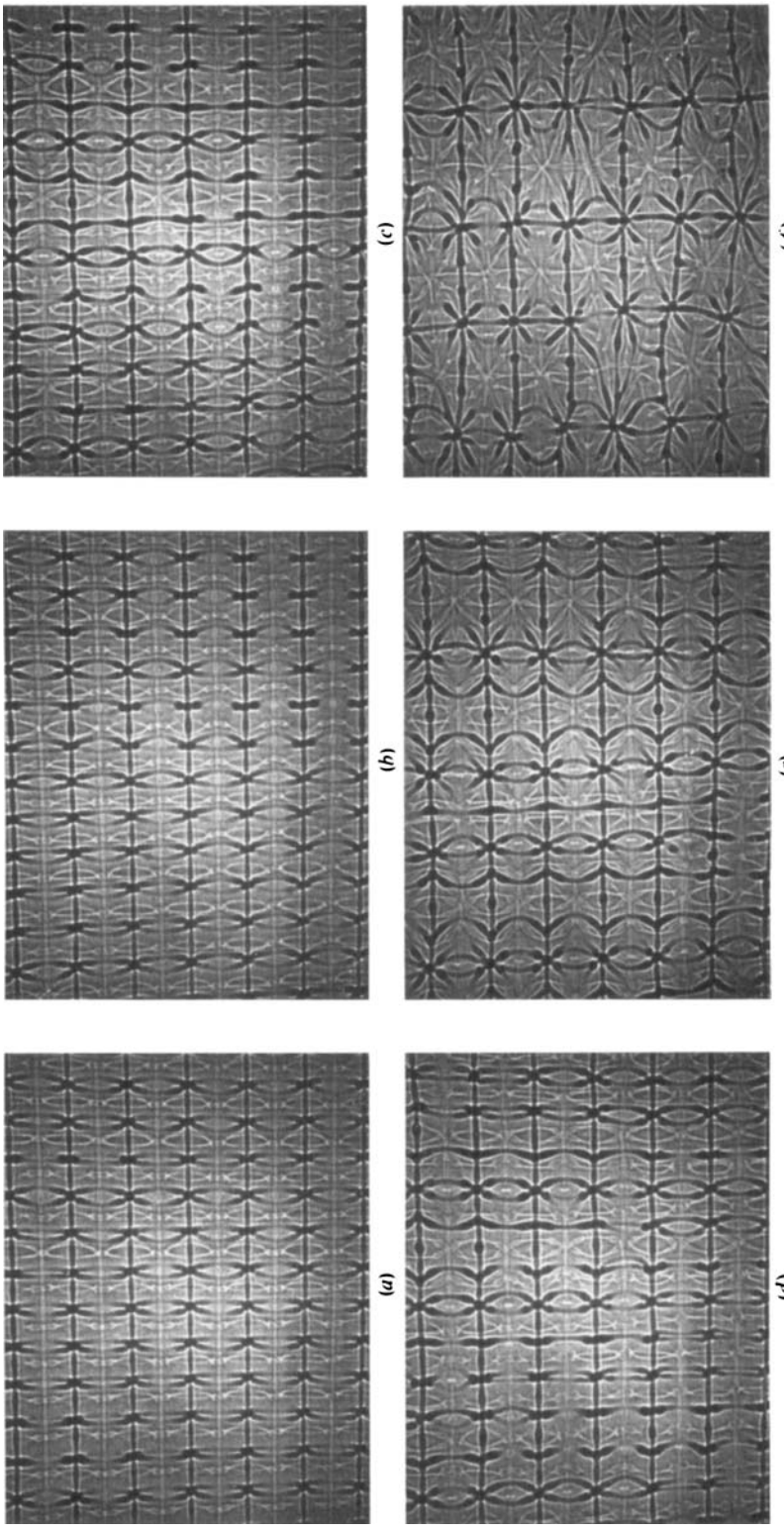

FIGURE 7. Oscillations of bimodal cells with wavenumbers $\alpha_1 = 2{\cdot}04$, $\alpha_2 = 4{\cdot}08$ and onset of collective instability for $P = 63$. Time intervals (min): (*a*)–(*b*) 0·67, (*b*)–(*c*) 8, (*c*)–(*d*) 0·40, (*d*)–(*e*) 6, (*e*)–(*f*) 17. During this time the Rayleigh number increases slightly from $1{\cdot}8 \times 10^5$ to $2{\cdot}0 \times 10^5$. (*a*), (*b*) and (*c*), (*d*) show approximately opposite phases of oscillation.

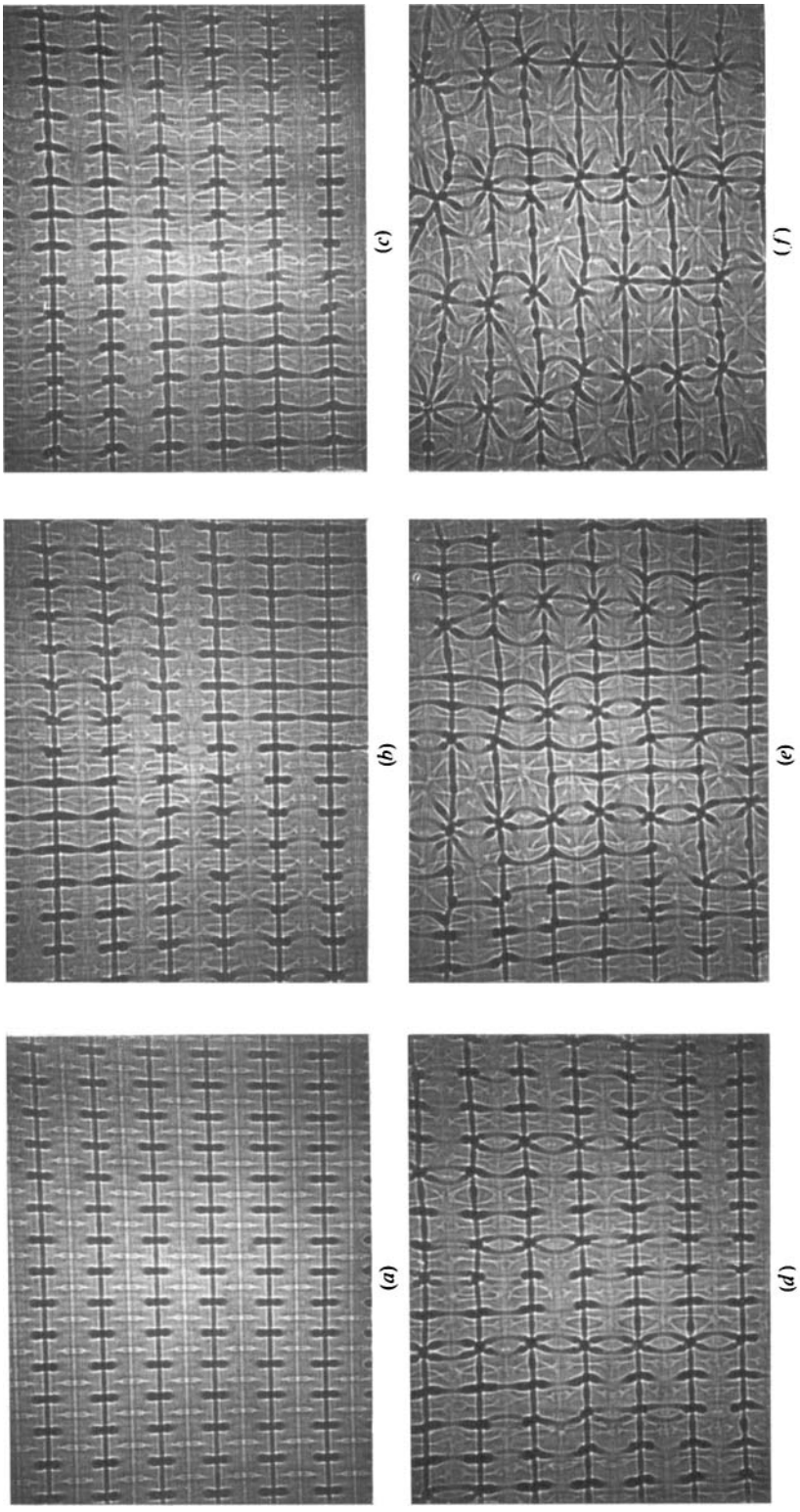

FIGURE 8. Oscillations of bimodal cells with wavenumbers $\alpha_1 = 2{\cdot}04$, $\alpha_2 = 4{\cdot}80$ and onset of collective instability for $P = 63$. Time intervals (min): (*a*)–(*b*) 11, (*b*)–(*c*) 0·25, (*c*)–(*d*) 13, (*d*)–(*e*) 14, (*e*)–(*f*) 21. The Rayleigh number was kept at $2{\cdot}0 \times 10^5$ except for (*a*), which was taken at $R = 1{\cdot}7 \times 10^5$. (*b*) and (*c*) show nearly opposite phases of oscillation.

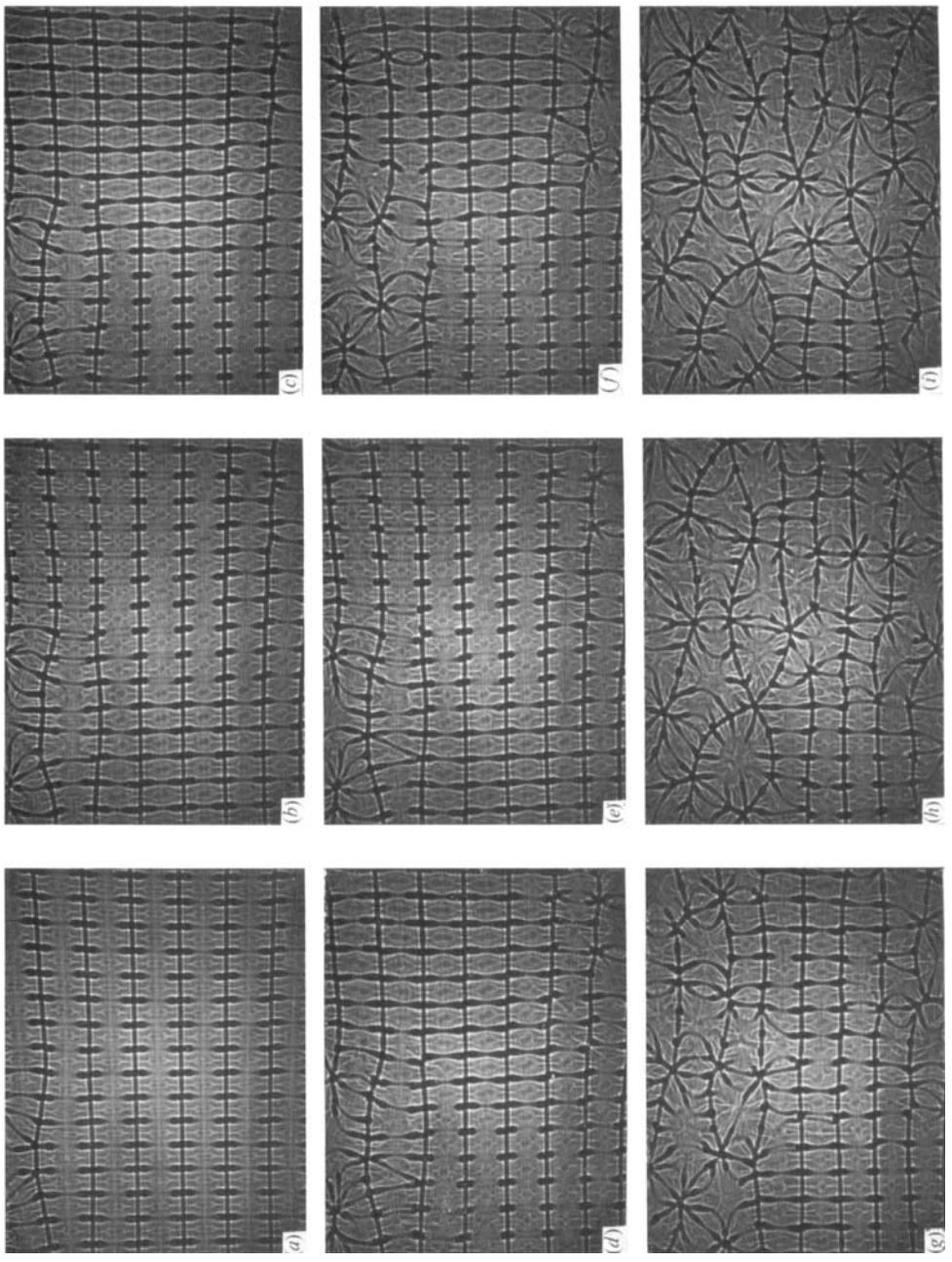

FIGURE 9. Onset of oscillations in bimodal cells with wavenumbers $\alpha_1 = 2{\cdot}04$, $\alpha_2 = 5{\cdot}45$ and irregular transition to spoke-pattern convection for $P = 63$. Time intervals (min): (*a*)–(*b*) 15, (*b*)–(*c*) 0·33, (*c*)–(*d*) 6, (*d*)–(*e*) 0·25, (*e*)–(*f*) 9, (*f*)–(*g*) 10, (*g*)–(*h*) 18, (*h*)–(*i*) 11. During this time the Rayleigh number was kept at $2{\cdot}4 \times 10^5$ except for (*a*), for which $R = 2{\cdot}2 \times 10^5$. (*b*), (*c*) and (*d*), (*e*) show approximately opposite phases of oscillation.

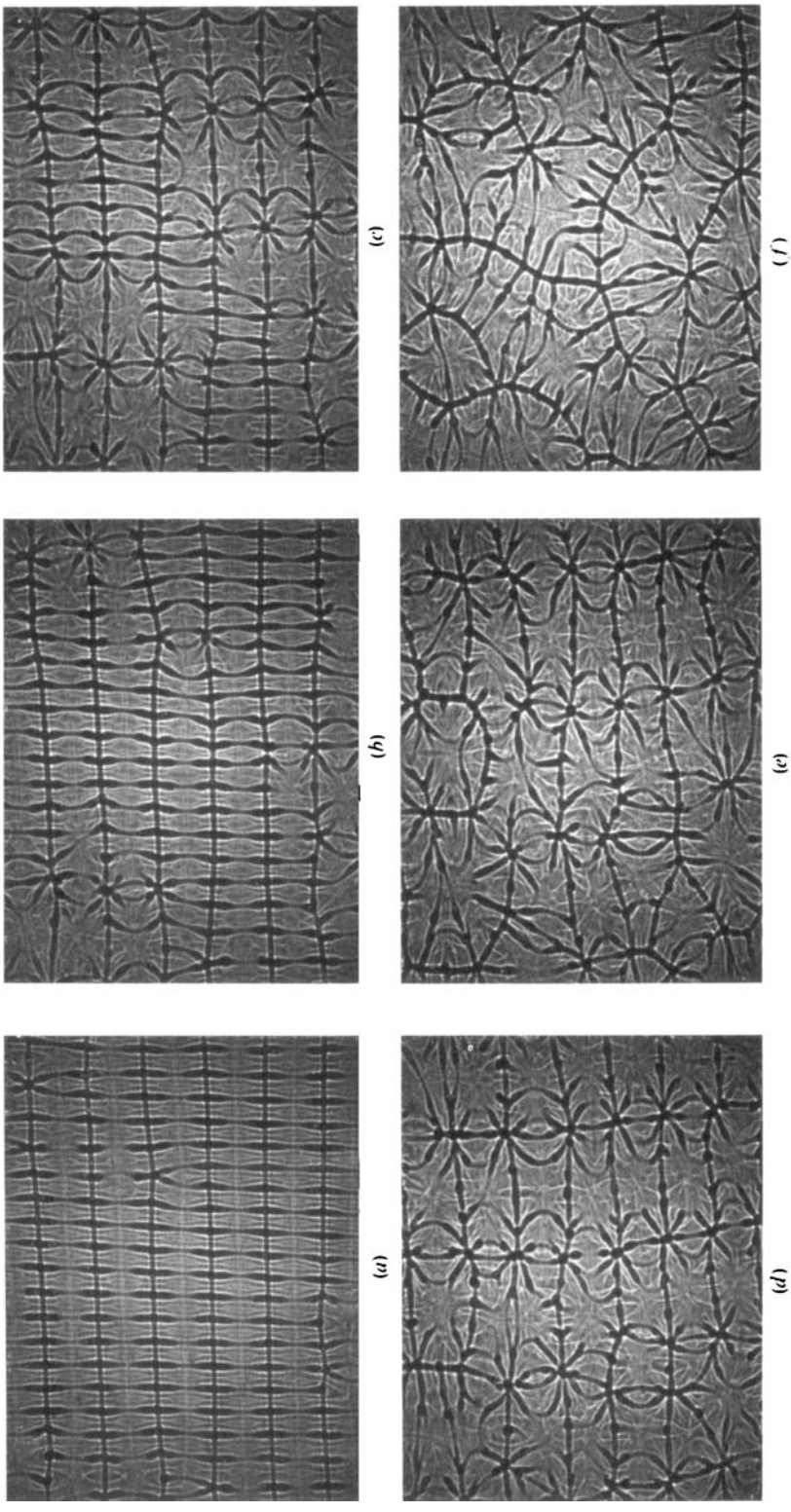

FIGURE 10. Irregular transition from bimodal convection with $\alpha_1 = 2{\cdot}04$, $\alpha_2 \approx 6{\cdot}0$ to spoke-pattern convection for $P = 63$. Time intervals (min): (*a*)–(*b*) 15, (*b*)–(*c*) 5, (*c*)–(*d*) 12, (*d*)–(*e*) 18, (*e*)–(*f*) 400. The Rayleigh number was kept at $2{\cdot}4 \times 10^5$ except for (*a*), which was taken at $R = 2{\cdot}1 \times 10^5$. The pattern of turbulent convection shown in (*f*) is essentially the same as in experiments started from random initial conditions.

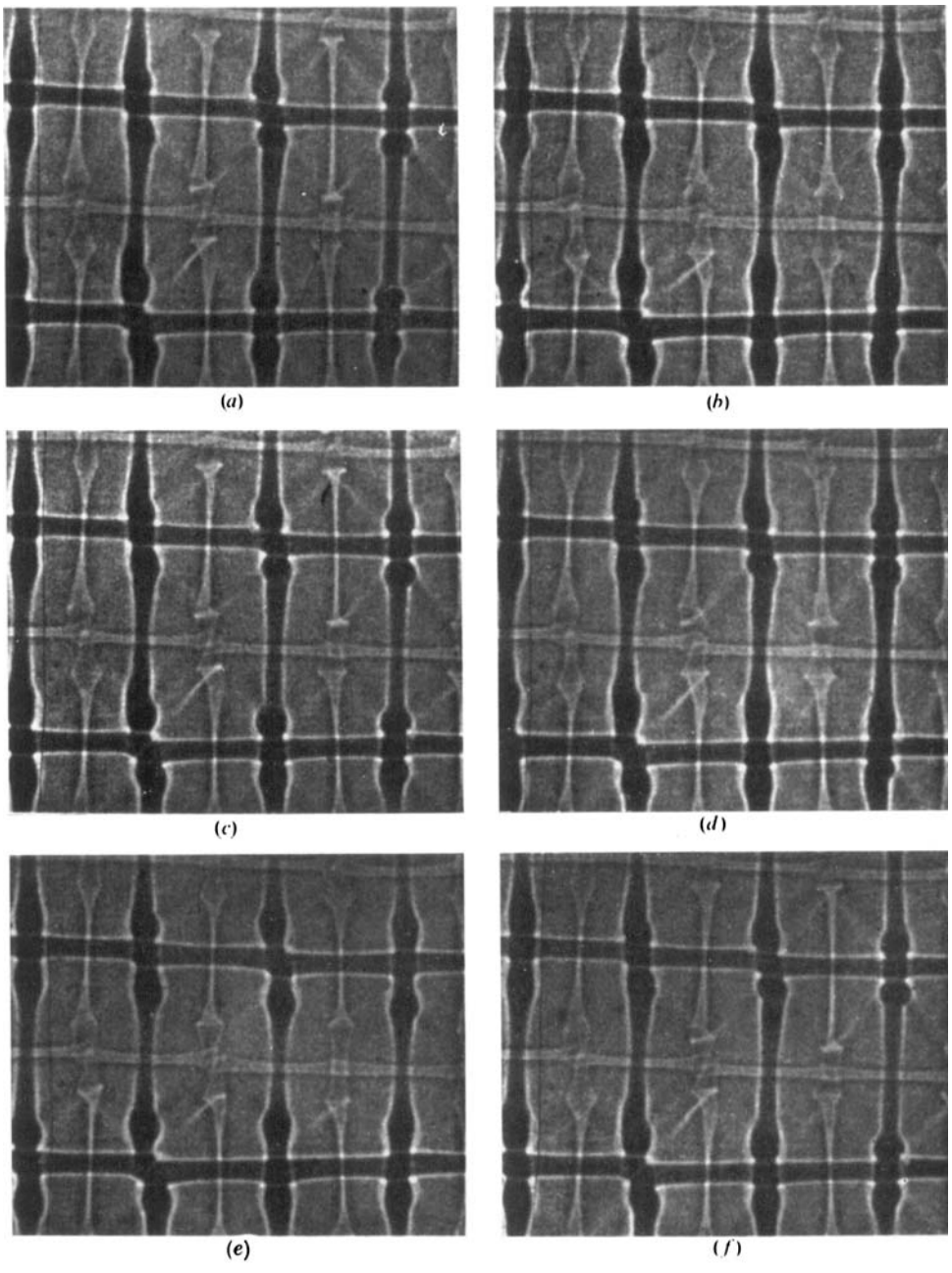

FIGURE 11. Prints from a 16 mm movie of oscillating bimodal convection in the case $P = 126$. Pictures were taken at 30 s intervals, corresponding to one complete cycle. The oscillation is best seen by following the pulsation of the light features in the centre of the cells and the dumbell-shaped boundaries, especially on the right side.